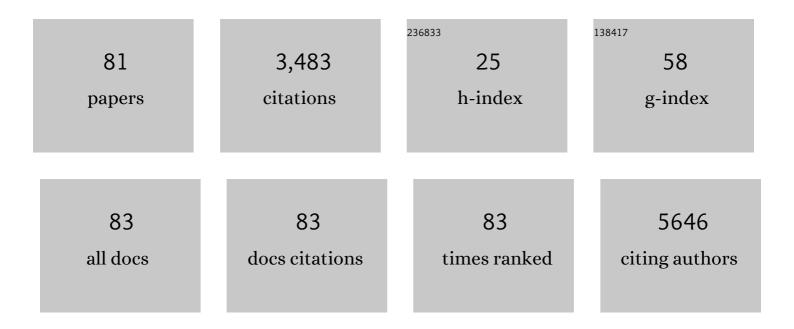
Jong-Min Yuk

List of Publications by Year in descending order

Source: https://exaly.com/author-pdf/4635010/publications.pdf Version: 2024-02-01



LONG-MIN YUK

#	Article	IF	CITATIONS
1	High-Resolution EM of Colloidal Nanocrystal Growth Using Graphene Liquid Cells. Science, 2012, 336, 61-64.	6.0	989
2	Raman Spectroscopy Study of Rotated Double-Layer Graphene: Misorientation-Angle Dependence of Electronic Structure. Physical Review Letters, 2012, 108, 246103.	2.9	486
3	3D structure of individual nanocrystals in solution by electron microscopy. Science, 2015, 349, 290-295.	6.0	238
4	Visualization of regulated nucleation and growth of lithium sulfides for high energy lithium sulfur batteries. Energy and Environmental Science, 2019, 12, 3144-3155.	15.6	104
5	Anisotropic Lithiation Onset in Silicon Nanoparticle Anode Revealed by <i>in Situ</i> Graphene Liquid Cell Electron Microscopy. ACS Nano, 2014, 8, 7478-7485.	7.3	103
6	Freeze-Dried Sulfur–Graphene Oxide–Carbon Nanotube Nanocomposite for High Sulfur-Loading Lithium/Sulfur Cells. Nano Letters, 2017, 17, 7086-7094.	4.5	95
7	In situ atomic imaging of coalescence of Au nanoparticles on graphene: rotation and grain boundary migration. Chemical Communications, 2013, 49, 11479.	2.2	93
8	Atomic visualization of a non-equilibrium sodiation pathway in copper sulfide. Nature Communications, 2018, 9, 922.	5.8	71
9	Heterojunction Based on Rh-Decorated WO ₃ Nanorods for Morphological Change and Gas Sensor Application Using the Transition Effect. Chemistry of Materials, 2019, 31, 207-215.	3.2	71
10	Growth dynamics of solid electrolyte interphase layer on SnO2 nanotubes realized by graphene liquid cell electron microscopy. Nano Energy, 2016, 25, 154-160.	8.2	63
11	Lithium Argyrodite Sulfide Electrolytes with High Ionic Conductivity and Air Stability for All-Solid-State Li-Ion Batteries. ACS Energy Letters, 2022, 7, 171-179.	8.8	61
12	Graphene Veils and Sandwiches. Nano Letters, 2011, 11, 3290-3294.	4.5	54
13	Extremely Stable Luminescent Crosslinked Perovskite Nanoparticles under Harsh Environments over 1.5 Years. Advanced Materials, 2021, 33, e2005255.	11.1	53
14	An iron-doped NASICON type sodium ion battery cathode for enhanced sodium storage performance and its full cell applications. Journal of Materials Chemistry A, 2020, 8, 20436-20445.	5.2	48
15	Graphene Liquid Cell Electron Microscopy: Progress, Applications, and Perspectives. ACS Nano, 2021, 15, 288-308.	7.3	45
16	Distinct handedness of spin wave across the compensation temperatures of ferrimagnets. Nature Materials, 2020, 19, 980-985.	13.3	42
17	Surface-normal electro-optic spatial light modulator using graphene integrated on a high-contrast grating resonator. Optics Express, 2016, 24, 26035.	1.7	39
18	Morphological Evolution Induced through a Heterojunction of W-Decorated NiO Nanoigloos: Synergistic Effect on High-Performance Gas Sensors. ACS Applied Materials & Interfaces, 2019, 11, 7529-7538.	4.0	39

Jong-Min Yuk

#	Article	IF	CITATIONS
19	Pulverizationâ€Tolerance and Capacity Recovery of Copper Sulfide for Highâ€Performance Sodium Storage. Advanced Science, 2019, 6, 1900264.	5.6	39
20	Real-Time Observation of Water-Soluble Mineral Precipitation in Aqueous Solution by In Situ High-Resolution Electron Microscopy. ACS Nano, 2016, 10, 88-92.	7.3	38
21	Reducing Time to Discovery: Materials and Molecular Modeling, Imaging, Informatics, and Integration. ACS Nano, 2021, 15, 3971-3995.	7.3	36
22	Electric-field control of field-free spin-orbit torque switching via laterally modulated Rashba effect in Pt/Co/AlOx structures. Nature Communications, 2021, 12, 7111.	5.8	36
23	Efficient preparation of graphene liquid cell utilizing direct transfer with large-area well-stitched graphene. Chemical Physics Letters, 2016, 650, 107-112.	1.2	32
24	High-rate formation cycle of Co3O4 nanoparticle for superior electrochemical performance in lithium-ion batteries. Electrochimica Acta, 2019, 295, 7-13.	2.6	32
25	Observation of Surface Atoms during Platinum Nanocrystal Growth by Monomer Attachment. Chemistry of Materials, 2015, 27, 3200-3202.	3.2	31
26	Cyclic tangential flow filtration system for isolation of extracellular vesicles. APL Bioengineering, 2021, 5, 016103.	3.3	31
27	Graphene-Sealed Flow Cells for <i>In Situ</i> Transmission Electron Microscopy of Liquid Samples. ACS Nano, 2020, 14, 9637-9643.	7.3	29
28	Efficient spin–orbit torque in magnetic trilayers using all three polarizations of a spin current. Nature Electronics, 2022, 5, 217-223.	13.1	28
29	Direct Realization of Complete Conversion and Agglomeration Dynamics of SnO ₂ Nanoparticles in Liquid Electrolyte. ACS Omega, 2017, 2, 6329-6336.	1.6	26
30	Direct Visualization of Lithium Polysulfides and Their Suppression in Liquid Electrolyte. Nano Letters, 2020, 20, 2080-2086.	4.5	26
31	Live Cell Electron Microscopy Using Graphene Veils. Nano Letters, 2020, 20, 4708-4713.	4.5	24
32	Stability of Plant Leaf-Derived Extracellular Vesicles According to Preservative and Storage Temperature. Pharmaceutics, 2022, 14, 457.	2.0	24
33	Machine learning assisted synthesis of lithium-ion batteries cathode materials. Nano Energy, 2022, 98, 107214.	8.2	24
34	Drastically increased electrical and thermal conductivities of Pt-infiltrated MXenes. Journal of Materials Chemistry A, 2021, 9, 10739-10746.	5.2	22
35	<i>In Situ</i> High-Resolution Transmission Electron Microscopy (TEM) Observation of Sn Nanoparticles on SnO ₂ Nanotubes Under Lithiation. Microscopy and Microanalysis, 2017, 23, 1107-1115.	0.2	21
36	Formation mechanism of ZnSiO3 nanoparticles embedded in an amorphous interfacial layer between a ZnO thin film and an n-Si (001) substrate due to thermal treatment. Journal of Applied Physics, 2008, 103, 083520.	1,1	20

Jong-Min Yuk

#	Article	IF	CITATIONS
37	Nucleation, growth, and superlattice formation of nanocrystals observed in liquid cell transmission electron microscopy. MRS Bulletin, 2020, 45, 713-726.	1.7	19
38	Liquidâ€Flowing Graphene Chipâ€Based Highâ€Resolution Electron Microscopy. Advanced Materials, 2021, 33, e2005468.	11.1	18
39	Unravelling high volumetric capacity of Co ₃ O ₄ nanograin-interconnected secondary particles for lithium-ion battery anodes. Journal of Materials Chemistry A, 2021, 9, 6242-6251.	5.2	18
40	Direct Fabrication of Zero- and One-Dimensional Metal Nanocrystals by Thermally Assisted Electromigration. ACS Nano, 2010, 4, 2999-3004.	7.3	16
41	Unveiling the Origin of Superior Electrochemical Performance in Polycrystalline Dense SnO ₂ Nanospheres as Anodes for Lithium-ion Batteries. ACS Applied Energy Materials, 2019, 2, 2004-2012.	2.5	14
42	Strong stress-composition coupling in lithium alloy nanoparticles. Nature Communications, 2019, 10, 3428.	5.8	13
43	Initial formation mechanisms of the supersaturation region and the columnar structure in ZnO thin films grown on n-Si (001) substrates. Applied Physics Letters, 2007, 90, 031907.	1.5	12
44	Superstructural defects and superlattice domains in stacked graphene. Carbon, 2014, 80, 755-761.	5.4	12
45	Boosted Zn ²⁺ storage performance of hydrated vanadium oxide by defect and heterostructure. Journal of Materials Chemistry A, 2022, 10, 13428-13438.	5.2	12
46	Formation mechanisms of metallic Zn nanodots by using ZnO thin films deposited on n-Si substrates. Applied Physics Letters, 2010, 97, 061901.	1.5	11
47	Graphene Liquid Cell Electron Microscopy of Initial Lithiation in Co ₃ O ₄ Nanoparticles. ACS Omega, 2019, 4, 6784-6788.	1.6	11
48	Transformation mechanisms from metallic Zn nanocrystals to insulating ZnSiO3 nanocrystals in a SiO2 matrix due to thermal treatment. Applied Physics Letters, 2008, 93, 221910.	1.5	10
49	Real-Time Observation of CaCO3Mineralization in Highly Supersaturated Graphene Liquid Cells. ACS Omega, 2020, 5, 14619-14624.	1.6	10
50	Protein-induced metamorphosis of unilamellar lipid vesicles to multilamellar hybrid vesicles. Journal of Controlled Release, 2021, 331, 187-197.	4.8	10
51	Enhancement of Photoresponse on Narrow-Bandgap Mott Insulator α-RuCl ₃ <i>via</i> Intercalation. ACS Nano, 2021, 15, 18113-18124.	7.3	10
52	Effect of nucleation density on the crystallinity of graphene grown from mobile hot-wire-assisted CVD. 2D Materials, 2019, 6, 011001.	2.0	9
53	Hollow Ag ₂ S nanosphere formation via electron beam-assisted oxidative etching of Ag nanoparticles. Chemical Communications, 2017, 53, 11122-11125.	2.2	8
54	Sequential Growth and Etching of Gold Nanocrystals Revealed by Highâ€Resolution Liquid Electron Microscopy. Physica Status Solidi (A) Applications and Materials Science, 2019, 216, 1800949.	0.8	7

Jong-Μin Yuk

#	Article	IF	CITATIONS
55	Evolution mechanisms of the surface morphology of grains in ZnO thin films grown on p-InP substrates due to thermal annealing. Applied Physics Letters, 2008, 93, .	1.5	6
56	Lithographically patterned well-type graphene liquid cells with rational designs. Lab on A Chip, 2020, 20, 2796-2803.	3.1	6
57	Atomic structural variations of [0001]-tilt grain boundaries during ZnO grain growth occurred by thermal treatments. Applied Surface Science, 2011, 257, 4817-4820.	3.1	5
58	Non-Equilibrium Sodiation Pathway of CuSbS ₂ . ACS Nano, 2021, 15, 17472-17479.	7.3	5
59	Functionalized Graphene as Cryo-EM Supporting Film. Microscopy and Microanalysis, 2018, 24, 882-883.	0.2	3
60	Preparation of Graphene Liquid Cells for the Observation of Lithium-ion Battery Material. Journal of Visualized Experiments, 2019, , .	0.2	3
61	Spontaneous stepwise formation of polar-facet-dominant ZnO crystals for enhanced catalytic H2O2 generation. Applied Surface Science, 2021, 561, 150061.	3.1	3
62	Effect of Thermal Annealing on the Formation of Preferential c-Axis Orientation and an Interfacial Layer for ZnO Thin Films Grown on an n-Si (001) Substrate. Journal of the Korean Physical Society, 2007, 50, 608.	0.3	3
63	Effects of thermal annealing on the microstructural properties of the lower region in ZnO thin films grown on n-Si (001) substrates. Journal of Materials Research, 2008, 23, 1082-1086.	1.2	2
64	In Situ TEM Observation on the Agglomeration of Nanoparticles in the Interface of SnO2. Microscopy and Microanalysis, 2017, 23, 2054-2055.	0.2	2
65	Preferential growth of carbon nanotubes via the carbon volume diffusion channels in Fe3C nanoparticles. Microscopy and Microanalysis, 2018, 24, 1884-1885.	0.2	2
66	Microscopic Insight into Tin Nanoparticle Magnesiation. ACS Applied Energy Materials, 2022, 5, 7944-7949.	2.5	2
67	The Effect of Electron Beam Dosage in the Decomposition Behavior of Electrolytes Encapsulated Inside the Graphene Sheets Based on In Situ TEM Observation. Microscopy and Microanalysis, 2017, 23, 2052-2053.	0.2	1
68	Enhanced self-assembly of block copolymers by surface modification of a guiding template. Polymer Journal, 2018, 50, 221-229.	1.3	1
69	Facile Fabrication of Graphene-Sealed Microwell Liquid Cell for Liquid Electron Microscopy. Microscopy and Microanalysis, 2018, 24, 298-299.	0.2	1
70	Facile <i>in situ</i> Lithiation and Sodiation Observation in TEM Employing MF (M=Li, Na). Microscopy and Microanalysis, 2019, 25, 1860-1861.	0.2	1
71	Hydrogen-Assisted Fast Growth of Large Graphene Grains by Recrystallization of Nanograins. ACS Omega, 2020, 5, 31502-31507.	1.6	1
72	Formation mechanisms of ZnO amorphous layers due to thermal treatment of ZnO thin films grown on pâ€InP (100) substrates. Journal of Applied Physics, 2008, 103, 083535.	1.1	0

JONG-ΜΙΝ ΥUK

#	Article	IF	CITATIONS
73	The creation of sub-10 nm In(PO3)3nanocrystals in an insulating matrix, and underlying formation mechanisms. Nanotechnology, 2009, 20, 055703.	1.3	0
74	Real Time Observation of Initial Conversion Reaction of Co3O4 Nanoparticles Using Graphene Liquid Cell Electron Microscopy. Microscopy and Microanalysis, 2017, 23, 1968-1969.	0.2	0
75	In situ Transmission Electron Microscopy of Lithiation Dynamics in a SnCh Hollow Nanosphere. Microscopy and Microanalysis, 2018, 24, 1944-1945.	0.2	0
76	Sodium Ion Batteries: Pulverizationâ€Tolerance and Capacity Recovery of Copper Sulfide for Highâ€Performance Sodium Storage (Adv. Sci. 12/2019). Advanced Science, 2019, 6, 1970074.	5.6	0
77	Electron Microscopy: Liquidâ€Flowing Graphene Chipâ€Based Highâ€Resolution Electron Microscopy (Adv.) Tj ET	Q _q 1_1 0.7	84314 rgBT
78	Perovskite Nanoparticles: Extremely Stable Luminescent Crosslinked Perovskite Nanoparticles under Harsh Environments over 1.5 Years (Adv. Mater. 3/2021). Advanced Materials, 2021, 33, 2170017.	11.1	0
79	Annealing Effects on the Microstructural Properties of the ZnO Thin Films Grown on p-InP (100) Substrates. Journal of the Korean Physical Society, 2008, 53, 357-360.	0.3	0
80	Annihilation Behavior of Planar Defects on Phosphorus-Doped Silicon at Low Temperatures. Journal of Nanoscience and Nanotechnology, 2017, 17, 3370-3374.	0.9	0
81	One-step synthesis of Pt/a-CoOx core/shell nanocomposites. Applied Microscopy, 2019, 49, 12.	0.8	0